Available online at www.sciencedirect.com
SCIENCE DIRECT
Polymer 47 (2006) 4075–4084
polymer
www.elsevier.com/locate/polymer

Organoclay degradation in melt processed polyethylene nanocomposites

Rhutesh K. Shah, D.R. Paul *

Department of Chemical Engineering and Texas Materials Institute, The University of Texas at Austin, Austin, TX 78712, USA

Available online 3 March 2006

Abstract

Melt processed nanocomposites were formed from low-density polyethylene, LDPE, and organoclays over a wide range of processing temperatures. These composites show limited exfoliation, and hence, their X-ray analysis reveals a distinct peak corresponding to the interplatelet distances in the unexfoliated clay galleries. The degradation of the quaternary ammonium surfactant of the organoclay in these systems was characterized by examining the change in the position of these peaks as a function of the melt processing temperature. Upon degradation, the mass of the surfactant within the clay galleries decreases, which causes the platelets to collapse and shifts the WAXS peak to lower *d*-spacings. The results of the WAXS analysis suggest that a significant portion of the surfactant is lost from the organoclays when the melt processing temperature is increased from 180 to 200 °C or higher. The extent of surfactant degradation in these composites was determined to be independent of the organoclay content. Organoclay degradation appears to limit the extent of exfoliation or dispersion in LDPE as revealed by stress–strain analyses of nanocomposites processed at different temperatures. The amount of surfactant lost during thermogravimetric analysis of various organoclays indicates that surfactants with multiple alkyl tails have greater thermal stability than those with a single alkyl tail. A comparison of the mass of surfactant lost during melt processing of nanocomposites and during thermogravimetric analysis of organoclays (in the absence of polymer) indicated that at a given time, a larger surfactant loss from the clay galleries occurs during extrusion than during the TGA experiment. This is attributed to the greater ease with which the degradation products (predominantly α-olefins) are solubilized in polyethylene for the composites as opposed to evaporated from the organoclay during TGA.

Keywords: Organoclay degradation; Nanocomposite; Polyethylene

1. Introduction

Polymer–clay nanocomposites continue to generate much interest, owing to their potential for exceptional improvements in properties at lower filler concentrations compared to conventional micro- and macro-composites. The key to achieving these benefits is exfoliating the clay into the polymer matrix to generate high aspect ratio particles. The first step in this direction is to make the hydrophilic smectite clay more organophilic using an ion exchange reaction between the naturally occurring alkali metal cations residing between aluminosilicate layers and alkyl ammonium surfactants to produce an 'organoclay'. Unfortunately, the currently used alkyl ammonium surfactants have low thermal stability and are known to degrade at the high temperatures required for melt processing most polymers. This could possibly affect the level of platelet exfoliation and perhaps interfacial bonding, which influence the physical and mechanical properties of the final nanocomposite. In addition, surfactant decomposition may also result in unwanted side reactions between the decomposition products and the polymer matrix, which could lead to matrix degradation and color formation in nanocomposites [1–4]. Xie et al. [5,6] have provided an extensive overview of the thermal degradation of alkyl quaternary ammonium modified montmorillonite clay. Their analysis of the degradation products using GC–MS indicated that the initial degradation of the surfactant in an organoclay follows a Hoffmann elimination reaction. VanderHart and Asano [7,8] estimated from NMR measurements that a considerable portion of the quaternary alkyl ammonium component is depleted during melt processing of nylon 6 nanocomposites. They concluded that the cause of the degradation is a combination of temperature and mechanical shear that is encountered during processing. Since melt processing seems to be one of the most convenient and attractive methods of producing nanocomposites, organoclay degradation during melt mixing has been the subject of recent attention in several laboratories [9–11].

* Corresponding author. Tel.: +1 512 471 5392; fax: +1 512 471 0542.
E-mail addresses: rhutesh@che.utexas.edu (R.K. Shah), drp@che.utexas.edu (D.R. Paul).

0032-3861/$ - see front matter © 2006 Elsevier Ltd. All rights reserved.
doi:10.1016/j.polymer.2006.02.031

The objective of this study is to examine thermal degradation of the surfactant in various organoclays using thermogravimetric analysis and 'insitu' in melt processed polyethylene–organoclay nanocomposites. Polyethylene, owing to its hydrophobic nature and lack of suitable interactions with the polar aluminosilicate surface of the clay, does not exfoliate organoclays efficiently. Transmission electron microscopy reveals an unexfoliated structure for nanocomposites prepared using one-tailed organoclays but a much better degree of dispersion, although not full exfoliation, for composites prepared using multiple tailed organoclays [12,13]. As a result, WAXS patterns of PE–organoclay nanocomposites exhibit a distinct peak confirming the presence of clay tactoids. In this work, we have characterized the level of organoclay degradation by examining the shift in the position of the WAXS peak of melt processed PE–organoclay nanocomposites. The low melting point of polyethylene allowed us to prepare nanocomposites over a wide range of temperatures (150–240 °C). The effect of surfactant degradation on the mechanical properties of nanocomposites prepared from one-tailed and two-tailed organoclays was determined by stress–strain analysis. Finally, the thermal stability of the three organoclays with different alkyl contents (number of alkyl tails) are compared by measuring the amount of surfactant lost during thermogravimetric analysis. The surfactant degradation observed while heating the organoclay (without polymer) is also compared to that seen in melt processed nanocomposites.

2. Experimental

2.1. Materials

Four commercial grades of LDPE were used in this study; their density and melt index values are listed in Table 1. Organoclays prepared by an ion exchange reaction between sodium montmorillonite (Na-MMT) and amine surfactants were supplied by Southern Clay Products, Inc. The selected organoclays are listed in Table 2 along with *d*-spacings determined by X-ray analysis and the cation exchange amount expressed as the milliequivalent ratio (MER). A nomenclature system, similar to that used in prior papers [14,15], has been adopted to describe the amine structure in a concise manner, i.e. M for methyl and HT for hydrogenated tallow (predominantly C_{18} chains). Procedural details of the cation exchange reaction between the onium ions and Na-MMT are provided by Fornes et al. [15].

The organoclays were carefully chosen to study the thermal stability of surfactants with varying number of alkyl tails. Also, our prior work [12–14] has shown that in polyethylene type matrices, organic modifiers with three long alkyl tails lead to higher levels of organoclay dispersion, and hence reinforcement, than those with two alkyl tails, which in turn result in better dispersion than organoclays with one-tail. Thus, the selected three organoclays also allow us to examine surfactant degradation, and its effects, in polyethylene nanocomposites with different morphologies.

2.2. Melt processing

Nanocomposites were prepared by melt mixing polymer pellets with organoclay powder in a Haake, co-rotating, intermeshing twin screw extruder (diameter = 30 mm, L/D = 10) using a screw speed of 280 rpm, and a feed rate of 1200 g/h. In order to examine the effect of processing temperature on surfactant degradation and mechanical properties of nanocomposites, LDPE (LD 621) was extruded with $M_3(HT)_1$ and $M_2(HT)_2$ organoclays at 150, 165, 180, 200, and 240 °C. The targeted montmorillonite (MMT) content in all nanocomposites was 5 wt%. Of course, such changes in the processing temperature also alter the polymer melt viscosity

Table 1
Polymers used in this study

Polyethylene grade	Supplier	Density (g/cm^3)	MI (dg/min)	Tensile modulus[a] (GPa)
LD 621	Exxon Mobil Chemical	0.919	1.9	0.121
Novapol LF-Y819-A	Nova Chemicals	0.919	0.75	0.142
Novapol LF-0219-A	Nova Chemicals	0.919	2.3	0.131
Novapol LC-0717-A	Nova Chemicals	0.917	7.0	0.110

[a] The tensile modulus was measured at room temperature according to ASTM D696.

Table 2
Organoclays used in this study

Organoclay	Chemical structure	Organic loading[a] (MER)	Organic content[b] (wt%)	d_{001} Spacing[c] (Å)
$M_3(HT)_1$	Trimethyl hydrogenated-tallow ammonium montmorillonite	95	29.6	18.0
$M_2(HT)_2$	Dimethyl bis(hydrogenated-tallow) ammonium montmorillonite	95	39.6	25.3
$M_1(C_{16})_3$	Methyl trihexadecyl ammonium montmorillonite	100	43.4	29.3

[a] The organic loading describes the number of milliequivalents of amine salt added per 100 g of clay (MER) during the cation exchange reaction with sodium montmorillonite.
[b] The wt% of organic component on the final organoclay was determined by high temperature residual ash measurements.
[c] The basal spacing corresponds to the characteristic Bragg reflection peak (d_{001}) obtained from a powder WAXS scan of the organoclay.

which could possibly affect organoclay exfoliation in these systems. To isolate the effect of these rheological variations on organoclay dispersion, it was first necessary to characterize the change in melt viscosity over the range of extrusion temperatures mentioned above. This was done in a Tinius Olsen melt indexer (extrusion plastometer) using a modified ASTM D1238 method. The ASTM standard test method for determining the melt index (MI) of the selected grade of polyethylene (LD 621) requires the melt flow rate to be measured at 190 °C under a 2.16 kg load. In our case, we measured the melt flow rate (g/10 min) of the polymer, LD 621 at several temperatures between 150 and 250 °C under a fixed load of 2.16 kg. Once the relation between the processing temperature and the melt flow rate of LD 621 was established, three grades of LDPE whose melt indices (MI), determined at the standard temperature of 190 °C, matched the high, low and intermediate points on the above curve were obtained from Nova Chemicals (Table 1). These three grades of polymer were then extruded with $M_2(HT)_2$ organoclay at 190 °C. Following extrusion, the amount of montmorillonite (MMT) in each nanocomposite was determined by placing pre-dried nanocomposite pellets in a furnace at 900 °C for 45 min and weighing the remaining MMT ash. A correction for loss of structural water is made in the calculation [19].

Tensile specimens (ASTM D638) were prepared by injection molding using an Arburg Allrounder 305-210-700 injection molding machine. To minimize differences in crystallization, all samples (irrespective of extrusion temperature) were injection molded under identical conditions: a barrel temperature of 150 °C, mold temperature of 45 °C, injection pressure of 40 bar and holding pressure of 40 bar. After molding, the samples were immediately sealed in a polyethylene bag and placed in a vacuum desiccator for a minimum of 24 h prior to testing.

2.3. Testing and characterization

WAXS was conducted at room temperature using a Sintag XDS 2000 diffractometer in the reflection mode with an incident X-ray wavelength of 1.542 Å at a scan rate of 1.0 °/min. X-ray analysis was performed on injection molded Izod bars except for the organoclays themselves which were in powder form. The Izod specimens were oriented such that the incident beam reflected off the major face.

Tensile tests were conducted at room temperature according to ASTM D696 using an Instron model 1137 machine equipped with digital data acquisition capabilities. An extensiometer was used to accurately measure the tensile modulus. As a result, the measurements were conducted at a crosshead speed of 0.51 cm/min as compared to the more conventional speed of 5.1 cm/min used for flexible materials. Typically, data from six specimens were averaged to determine the tensile modulus with standard deviation in the range of 1–5%.

Isothermal thermogravimetric analysis (TGA) was conducted on pure organoclays using a Perkin–Elmer TGA7 at 150, 180, 200, 220, and 240 °C under both air and nitrogen atmospheres at a gas flow rate of 50 mL/min. according to ASTM E1131. All organoclays were dried overnight under vacuum at 80 °C prior to thermal analysis.

3. Results

3.1. Organoclay degradation characterized by WAXS analysis

Fig. 1(a) shows the WAXS scans of nanocomposites prepared by melt mixing LDPE (LD 621) and $M_3(HT)_1$ organoclay at various temperatures; the presence of a distinct peak indicates incomplete exfoliation of the clay platelets as would be expected [12,13]. The WAXS pattern of pristine $M_3(HT)_1$ organoclay, which reveals an intense peak corresponding to a basal spacing of 18 Å, is also included for comparison. It is interesting to note the change in the position of the X-ray scattering intensity peak for the nanocomposites as the processing temperature is increased. For composites extruded at 150 and 165 °C, the peak position remains the

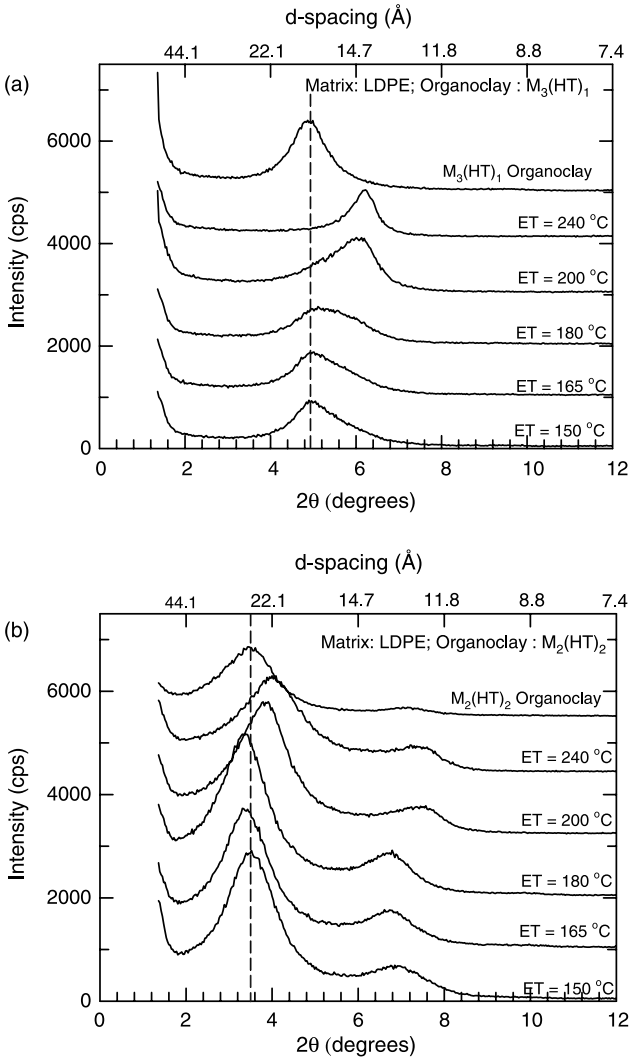

Fig. 1. WAXS patterns of injection molded samples of LDPE nanocomposites prepared from (a) $M_3(HT)_1$ and (b) $M_2(HT)_2$ organoclays at various extrusion temperatures (ET). X-ray scans of the organoclays are also plotted for comparison. The concentration of MMT in all cases is about 5 wt%. The curves are shifted vertically for clarity.

same as that of the pristine organoclay, which suggests that in these systems the interplatelet distance of the organoclay does not change much during melt processing. The scattering peak for nanocomposites extruded at 180 °C is broader, and shifts a little to the right which denotes a slight decrease in the interplatelet spacing of the organoclay and could be interpreted as the early stages of surfactant degradation resulting in a loss of mass from the organoclay galleries. On increasing the melt processing temperature from 180 to 200 °C, there is a distinct shift in the peak position as the organoclay *d*-spacing is reduced dramatically to ~14 Å. It appears that a significant portion of the surfactant is lost from the clay galleries between 180 and 200 °C. On further increasing the processing temperature to 240 °C, the position of the peak does not change much suggesting that the clay galleries do not collapse any further. However, the breadth of the peak reduces which could be construed as more uniform organoclay degradation as compared to that observed in nanocomposites processed at 200 °C.

WAXS scans of nanocomposites prepared by melt mixing LDPE and $M_2(HT)_2$ organoclay at various temperatures are presented in Fig. 1(b). As in the case of LDPE-$M_3(HT)_1$ composites, the peak position for LDPE-$M_2(HT)_2$ nanocomposites processed at 150 °C remains the same as that of the pristine organoclay (25.3 Å). The peak shifts to ~23.2 Å when the processing temperature is increased to 200 °C. Increasing the processing temperature further to 240 °C results in a further decrease in the organoclay *d*-spacing (~22 Å) indicative of an increased loss of mass from the galleries. Careful observation of the WAXS patterns of composites processed at 165 and 180 °C reveals a shift to the left relative to that of the pristine organoclay which is often interpreted as a sign of polymer intercalation within the clay galleries. However, we do not think this is the only explanation. The increased *d*-spacing could also result from intercalation of the low molecular weight oligomers that may be present within the matrix polymer. An alternative explanation derived from studies exploring the density and molecular packing of surfactants within the organoclay galleries should also be considered. Based upon molecular simulations and experimental results, Paul et al. [16] suggested that within an organoclay gallery, the head (nitrogen) groups of the surfactant are essentially tethered to the clay surface while the long hydrocarbon chains tend to adopt a layering structure with disordered conformation. The density of the surfactant in the gallery was determined to be higher than typical of organics of this type which was attributed to the restrictions on molecular motions due to tethering. In the current experiments, as the melt processing temperature increases, the surfactant molecules begin to degrade; however, the alkyl tails which become detached from the ammonium ion may not be immediately extracted from the clay galleries. The detached tails and other degradation products have larger degrees of freedom than surfactant molecules ionically attached to the clay surface. This coupled with the increased energy arising from the higher temperatures could result in some expansion of the organoclay galleries. Why such a shift to the left is observed for nanocomposites based on the $M_2(HT)_2$ organoclay but not the $M_3(HT)_1$ organoclay is not completely understood. The $M_2(HT)_2$ organoclay has a higher mass ratio of intercalated surfactant to clay than the $M_3(HT)_1$ organoclay (0.55 versus 0.33) [16]. As described later, the two organoclays exhibit different degrees of thermal stability and different levels of exfoliation in LDPE. The effects of these factors on the phenomenon mentioned above have not been fully explored yet. Yoon et al. [17] observed a similar shift to the left in WAXS profiles of pristine $M_2(HT)_2$ organoclay that was heated in a compression molding press in the absence of any polymer. In all cases, the d_{002} peaks, observed at a $2\theta \sim 7°$, shift in the same direction and to the same extent as the d_{001} peaks.

Fig. 2 compares the WAXS patterns of nanocomposites prepared from LDPE and varying amounts of organoclay. As expected, for both the $M_3(HT)_1$ and $M_2(HT)_2$ based organoclays, the X-ray scattering intensity increases as the montmorillonite content increases. However, the position of the peak does not change with the organoclay content. Thus, it seems that the extent of surfactant degradation in these

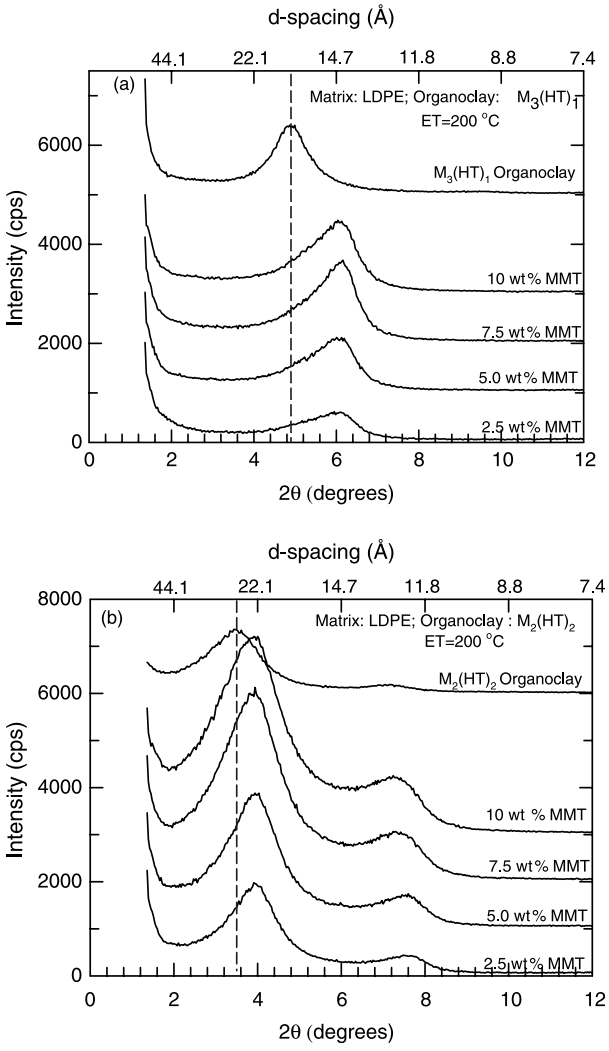

Fig. 2. WAXD patterns of injection molded samples of LDPE nanocomposites with different montmorillonite contents prepared from (a) $M_3(HT)_1$ and (b) $M_2(HT)_2$ organoclays. The extrusion temperature (ET) in all cases is 200 °C. The curves are shifted vertically for clarity.

nanocomposites is essentially independent of the organoclay content. The color of the injection molded nanocomposite samples varied from pale yellow to dark brown depending upon their clay content, and the extrusion temperatures used to prepare them. In general, the intensity of the color increased as the clay content and/or extrusion temperatures used to make the nanocomposites increased.

3.2. Effect of organoclay degradation on mechanical properties

The relative improvement in matrix stiffness achieved by melt mixing LDPE with $M_3(HT)_1$ and $M_2(HT)_2$ organoclays at various temperatures is presented in Fig. 3. The montmorillonite content of the nanocomposites was controlled between 4.95 and 5.1 wt% (based upon measurement of ash content as described in Section 2). Nanocomposites prepared from $M_2(HT)_2$ organoclay exhibit higher levels of reinforcement than those prepared from $M_3(HT)_1$ organoclay at all extrusion temperatures. Similar observations were made in prior studies [12–14], where it was determined that the larger the number of alkyl tails on the organic modifier, the higher the level of organoclay exfoliation in polyethylene. The TEM analysis paralleled the mechanical property trends observed in those studies. The TEM micrographs expressly revealed a partially exfoliated morphology for polyethylene–$M_2(HT)_2$ nanocomposites and an unexfoliated structure for polyethylene–$M_3(HT)_1$ composites.

The tensile modulus of nanocomposites prepared from $M_3(HT)_1$ organoclay seems to be essentially unaffected by the melt processing temperature. It appears that the one-tailed surfactant results in such poor organoclay–polymer interactions that the extent of organoclay dispersion, and hence reinforcement, is independent of the degree of surfactant degradation. On the other hand, the modulus of $M_2(HT)_2$ based nanocomposites drops steadily when the processing temperature is increased beyond 165 °C. As expected, the increase in processing temperature is also accompanied by a drop in the

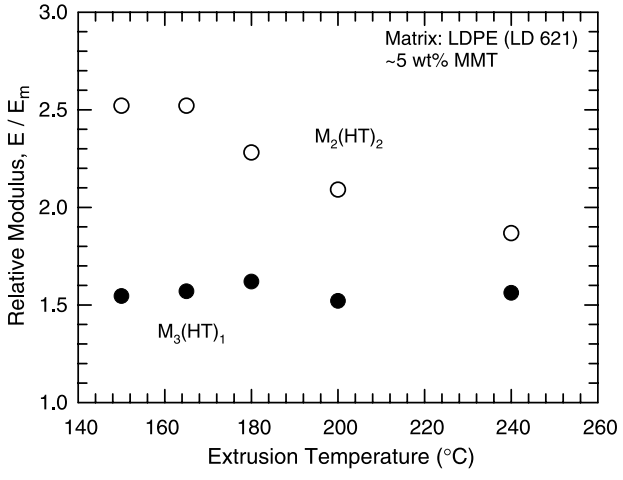

Fig. 3. Relative modulus (E/E_m) as a function of the extrusion temperature for LDPE (LD 621) nanocomposites prepared from $M_3(HT)_1$ and $M_2(HT)_2$ organoclays. The concentration of MMT in all cases is about 5 wt%.

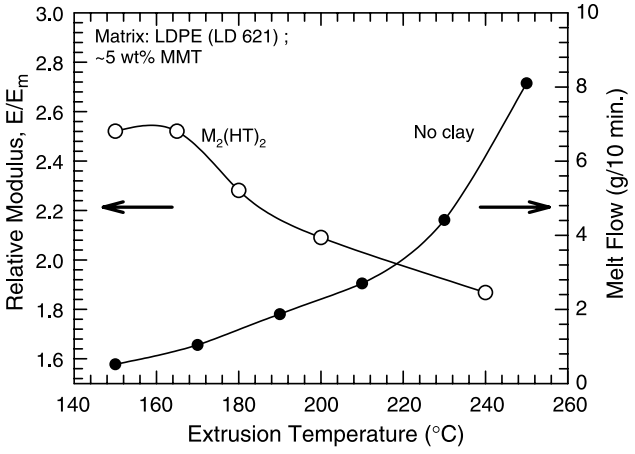

Fig. 4. Relative modulus (E/E_m) of LD 621-$M_2(HT)_2$ nanocomposites (left axis) is plotted as a function of the extrusion temperature. The data for the melt flow rate of LD 621 (right axis) is plotted against temperature to demonstrate the change in the melt viscosity of the matrix polymer over the same range of temperature.

polymer melt viscosity. Our melt processing studies with nylon 6 nanocomposites have revealed that high molecular weight grades of nylon 6 lead to higher levels of exfoliation of organoclays, owing to their higher melt viscosity, than do low molecular weight grades of nylon 6 [18,19]. Hence, one could argue, that the drop observed in the tensile modulus of LDPE–$M_2(HT)_2$ nanocomposites with the increase in processing temperature might be a result of the reduction in polymer melt viscosity with temperature. To isolate any rheological effects on exfoliation, it was first necessary to characterize the change in melt viscosity over the range of extrusion temperatures mentioned above. As explained in Section 2, this was accomplished using a melt indexer (extrusion plastometer). The melt flow rate (g/10 min) of the polymer, LD 621 was measured at several temperatures between 150 and 250 °C under a fixed load of 2.16 kg and the results are presented in Fig. 4. The curve shows the melt flow rate to increase from 0.25 g/10 min at 150 °C to 6.2 g/10 min at 240 °C. To account for these changes in melt viscosity, three grades of LDPE with melt indices of 0.75, 2.3 and 7.0, respectively, and similar densities were extruded with the same $M_2(HT)_2$ organoclay at 190 °C. The relative increase in tensile modulus, due to reinforcement by the clay, achieved using LDPE resins of different melt indices is presented in Fig. 5. If the high melt viscosity polymer (within the range mentioned above) caused the improved exfoliation of the selected organoclay, the nanocomposites prepared from Novapol LF-Y819-A (0.75 MI) would have resulted in higher levels of reinforcement than those prepared from Novapol LC-0717-A (7.0 MI). That does not seem to be the case. Although there are minor differences in the montmorillonite content of the nanocomposites (4.84–5.13 wt% instead of the targeted 5.0 wt%), it seems that for the MI range mentioned above, the tensile modulus is essentially independent of the polymer melt viscosity, or, if anything, the relative modulus increases with the melt index. Thus, it would be safe to conclude that the drop in the relative modulus of the LDPE–$M_2(HT)_2$ nanocomposites processed at high

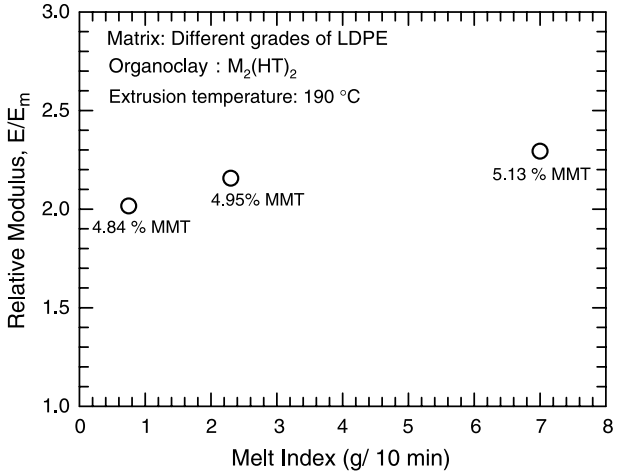

Fig. 5. Relative modulus (E/E_m) of LDPE–$M_2(HT)_2$ nanocomposites as a function of the melt index of the matrix polymers from which they are formed. Note that there are slight differences in MMT content in the materials that partly account for the trend shown.

temperatures (Fig. 4) is entirely a result of the increased level of surfactant degradation at those temperatures. It appears that the extraction of the organic modifier from the clay galleries and the subsequent reduction of the organoclay *d*-spacing hampers the ability of LDPE to disperse the $M_2(HT)_2$ organoclay into high aspect ratio particles.

3.3. Thermogravimetric analysis (TGA) of pristine organoclays

The thermal stability of the three organoclays with different number of alkyl tails was compared using thermogravimetric analysis. First, the effect of the purge gas on surfactant mass loss was evaluated. Fig. 6 compares the thermograms of $M_3(HT)_1$ organoclay obtained at 200 °C using nitrogen and air. The data are presented in terms of fractional mass loss of the surfactant rather than the fractional loss of the mass of organoclay. There is slightly more degradation in air than in nitrogen but the difference between the two curves is relatively small. Thus, the degradation is mainly thermally driven with perhaps a slight oxidative contribution. A previous study [10] reported similar observations during thermogravimetric analysis of a two-tailed organoclay (for $T \leq 200$ °C). Since the choice of purge gas used does not significantly affect the amount of surfactant lost, nitrogen gas was arbitrarily chosen as the purge medium for these analyses. Fig. 7 shows the isothermal plots of mass loss versus time for the one-tailed

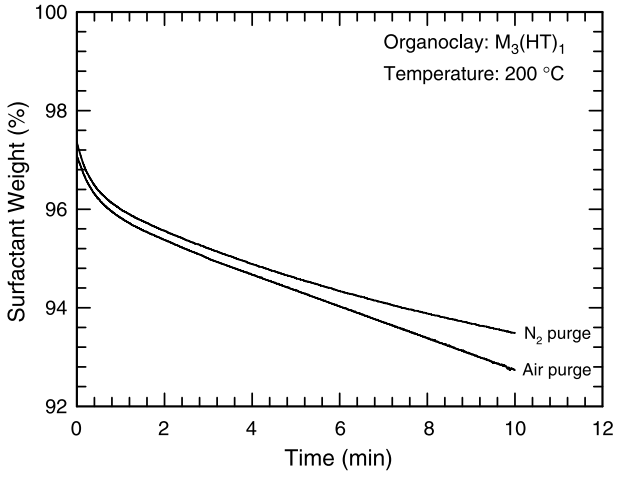

Fig. 6. Isothermal TGA results for pre-dried $M_3(HT)_1$ organoclay obtained in air and nitrogen at 200 °C.

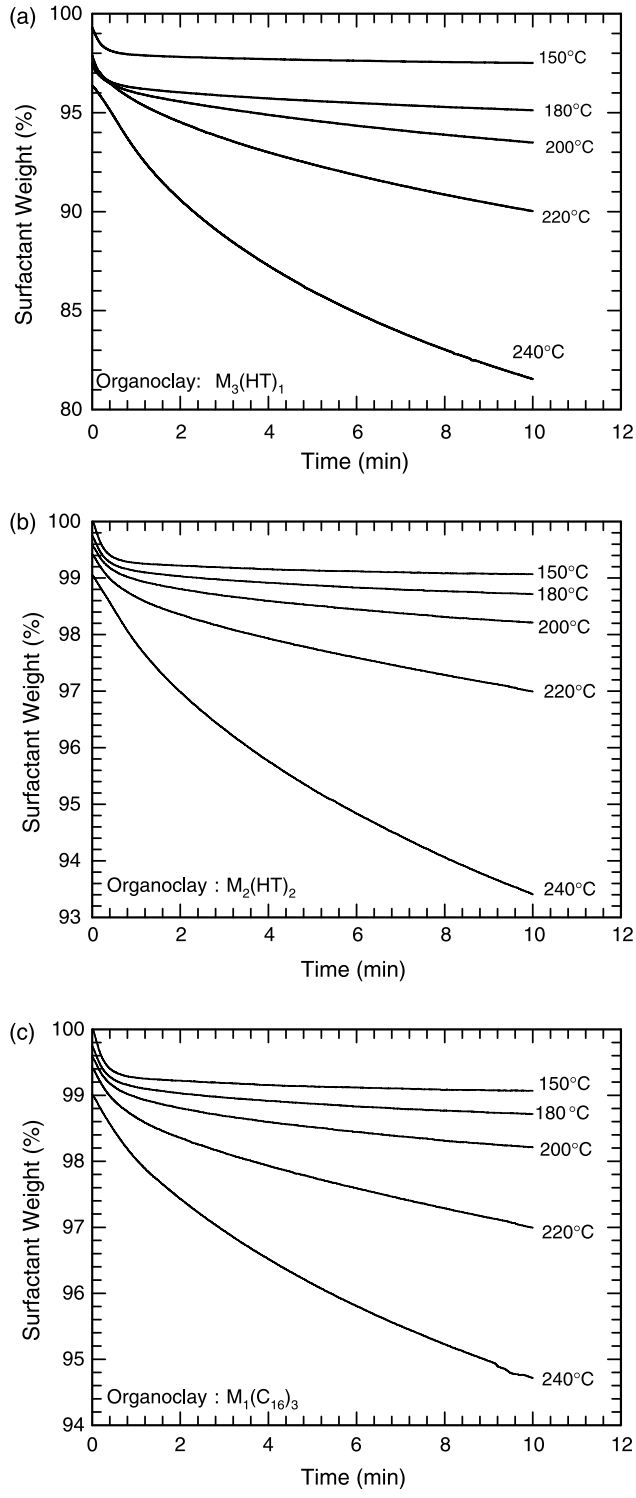

Fig. 7. Isothermal TGA results of (a) $M_3(HT)_1$, (b) $M_2(HT)_2$ and (c) $M_1(C_{16})_3$ organoclays obtained in nitrogen at various temperatures.

($M_3(HT)_1$), two-tailed ($M_2(HT)_2$), and three-tailed ($M_1(C_{16})_3$) organoclays conducted over a wide range of temperatures (150–240 °C). As expected, for all organoclays, the extent of mass loss increases as the test temperature becomes higher; however, the rate of surfactant loss increases dramatically in going from 200 to 220 °C. The rate of mass loss increases even more rapidly when the test temperature is raised to 240 °C. Gelfer et al. [10] noticed a similar trend for two-tailed organoclays. They observed very little surfactant loss between 100 and 200 °C. The major weight loss began at 200 °C and continued until 400 °C.

Interestingly, the rate of mass loss for a one-tailed organoclay ($M_3(HT)_1$) is greater than for the multiple-tailed organoclays under the same testing conditions; note the more expanded scales in Fig. 7(b) and (c) than in Fig. 7(a). This is further elucidated in Fig. 8 where the weight fraction of the surfactant remaining is plotted against time for the three organoclays at 150, 200 and 240 °C. At all three temperatures, $M_1(C_{16})_3$ seems to be more thermally stable than $M_2(HT)_2$ which in turn is more stable than $M_3(HT)_1$. The difference between the weight fraction of the surfactant lost in the $M_3(HT)_1$ and the $M_2(HT)_2$ organoclay is much larger than the difference between $M_2(HT)_2$ and $M_1(C_{16})_3$ organoclays. A similar observation was made by Osman et al. [9] while comparing the thermal stability of various organoclays at 200 °C. In their study, organoclays based on dioctadecyldimethylammonium required a longer time to register the same percentage drop in surfactant content than for octadecyltrimethylammonium based organoclays.

It should be remembered that the $M_1(C_{16})_3$ organoclay has a higher organic content than the $M_2(HT)_2$ organoclay which in turn has a higher organic content than the $M_3(HT)_1$ organoclay (Table 2). Thus, a comparison of the reduction in surfactant content in the three given organoclays does not offer a clear comparison of the absolute amount of surfactant leaving the clay galleries during TGA. To resolve this, we have plotted in Fig. 9 the absolute mass loss normalized by the montmorillonite content of each sample for the three organoclays during isothermal TGA at 150, 200 and 240 °C. The trends observed are similar to those presented in Fig. 8; despite having a larger alkyl content, $M_2(HT)_2$ and $M_1(C_{16})_3$ organoclays lose less mass than the one-tailed, $M_3(HT)_1$ organoclay. All these observations lead us to the conclusion that organoclays prepared from ammonium-based surfactants with multiple alkyl tails have greater thermal stability than those with a single alkyl tail.

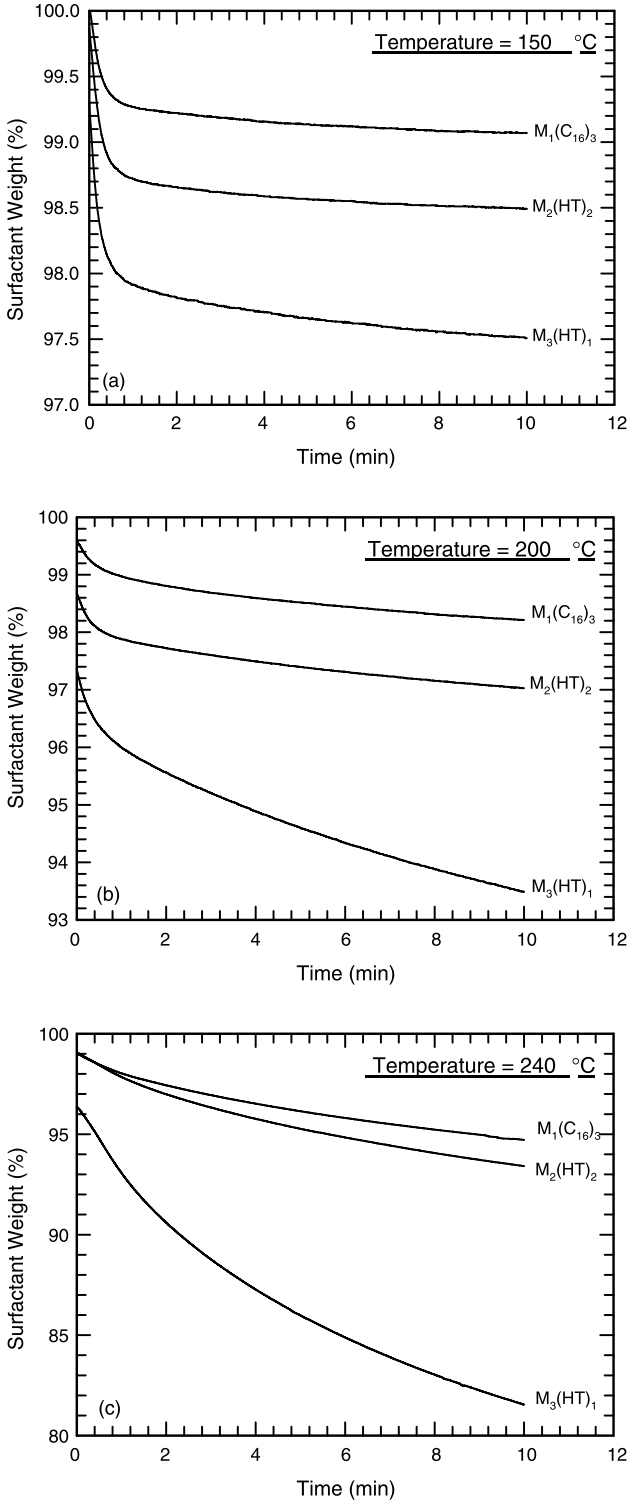

Fig. 8. Isothermal TGA results showing the weight percent of surfactant loss from $M_3(HT)_1$, $M_2(HT)_2$ and $M_1(C_{16})_3$ organoclays at (a) 150 °C, (b) 200 °C and (c) 240 °C under nitrogen atmosphere.

4. Discussion

The amounts of surfactant lost from $M_3(HT)_1$ organoclay during nanocomposite extrusion and during thermogravimetric analysis of the organoclay at 200 and 240 °C are listed in Table 3. The amount of surfactant leaving the clay galleries during nanocomposite extrusion was calculated from the reduction in the *d*-spacing of the melt processed composites. A few approximations were necessary to allow these calculations. First, the surfactant density was assumed to be uniform across the interplatelet region. It was also assumed that there is no intercalation of LDPE within the $M_3(HT)_1$ organoclay galleries. Based upon the TEM analysis of LDPE–$M_3(HT)_1$ organoclay nanocomposites presented elsewhere [12,13], this assumption seems to be appropriate. The average

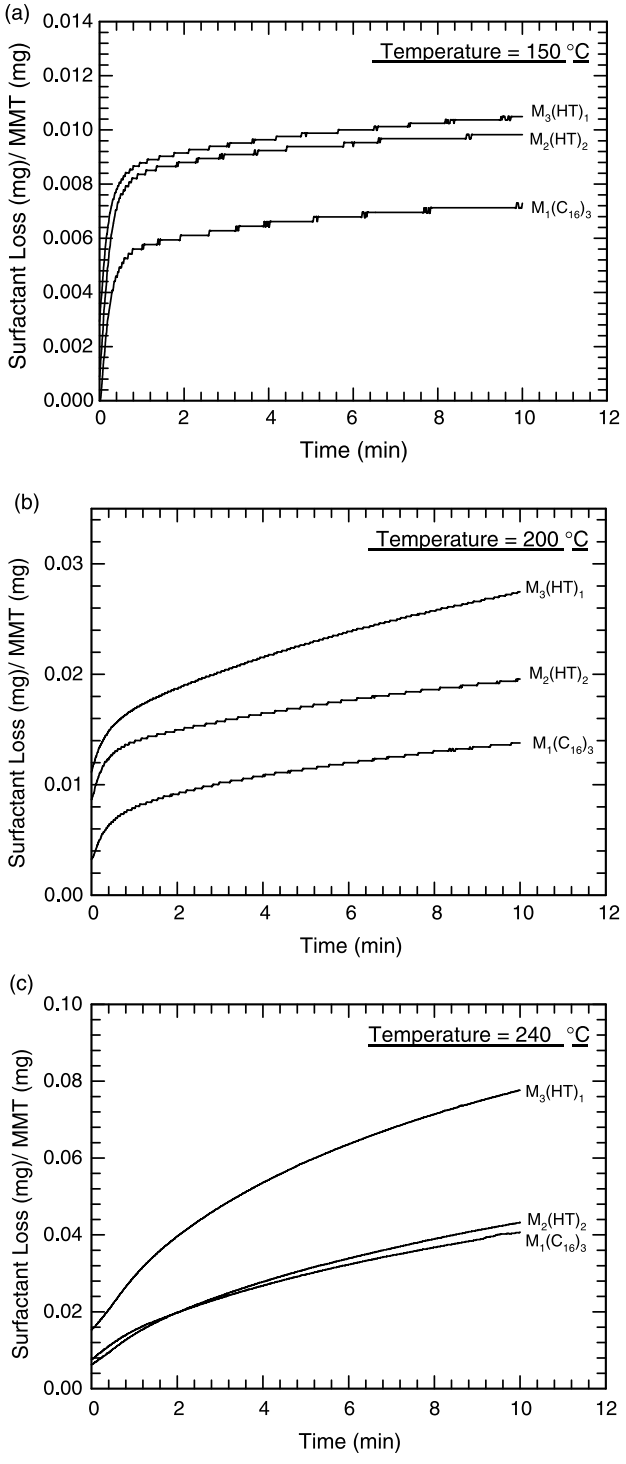

Fig. 9. Isothermal TGA results showing the absolute mass loss for $M_3(HT)_1$, $M_2(HT)_2$ and $M_1(C_{16})_3$ organoclays at (a) 150 °C, (b) 200 °C and (c) 240 °C under nitrogen atmosphere.

polymer residence time in the extruder used for this study has been determined to be 3.4 min [2,20]. Hence, in order to ensure a fair comparison, surfactant weight loss during thermogravimetric analysis was calculated at 3.4 min and 10 min using air as purge gas. This comparison is presented graphically in Fig. 10. The data clearly reveal a larger amount of surfactant loss from the clay galleries during melt processing than during TGA. Xie et al. [5] analyzed the degradation products released during the thermogravimetric analysis of trimethyloctadecyl ammonium chloride organoclays ($M_3(C_{18})_1$) using a GC–MS technique. Their analysis suggested that the initial degradation of the organoclay follows a Hoffman elimination mechanism (shown below for alkyl ammonium hydroxide) with the release of long chained α-olefins (C16–C18). Alternative schemes for Hoffman elimination reaction for organically modified montmorillonite are also available in the literature [2,11]. All of them suggest the formation of alpha olefins, amines and other products resulting from the secondary reactions between the degradation products within the organoclay.

Table 3
Amount of surfactant loss from $M_3(HT)_1$ organoclay during nanocomposite extrusion and thermogravimetric analysis of the organoclay

	Melt processing			Thermogravimetric analysis	
Temperature (°C)	WAXD peak position	Change in peak position[a] (Å)	Surfactant loss[b] (Å)	Surfactant loss at $t=$ 3.4 min[c] (wt%)	Surfactant loss at $t=$ 10 min (wt%)
200	14.7	3.3	38.4	5.1	7.3
240	14.2	3.8	44.2	12.3	19.4

[a] Calculated using a peak position of 18 Å for pristine $M_3(HT)_1$ organoclay.
[b] Based upon a thickness of 9.4 Å for an aluminosilicate platelet, exclusive of the sodium ion, and assuming (i) uniform surfactant density between the platelets, and (ii) no polymer intercalation within the clay galleries.
[c] The average residence time for the extruder used in this study was 3.4 min [2,20].

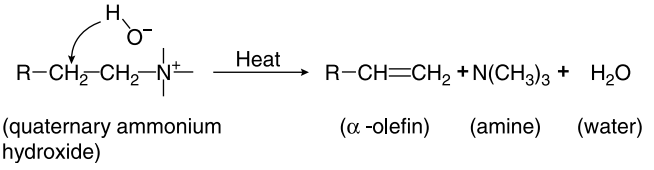

The primary mechanism by which these degradation products leave the clay galleries during TGA would be by

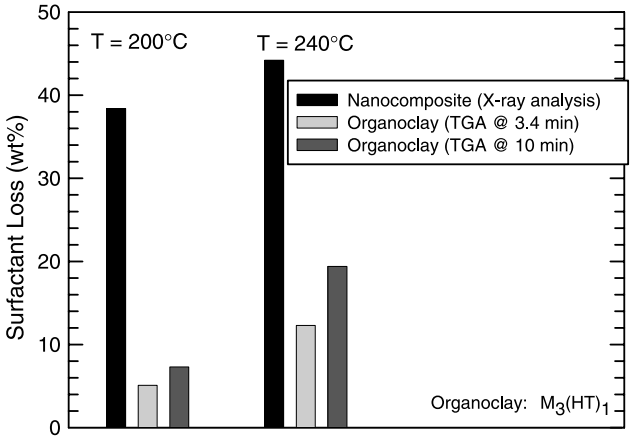

Fig. 10. Comparison of the surfactant loss from $M_3(HT)_1$ organoclay during nanocomposite extrusion and during thermogravimetric analysis of the organoclay at 200 and 240 °C.

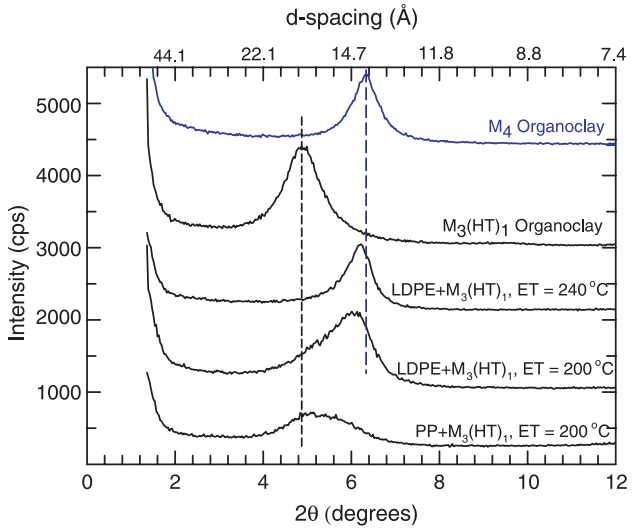

Fig. 11. WAXD patterns of injection molded samples of LDPE and polypropylene nanocomposites prepared from $M_3(HT)_1$ organoclay at 200 and 240 °C. X-ray scans of $M_3(HT)_1$ and M_4 (tetra methyl ammonium) organoclays are plotted for comparison. The concentration of MMT in all cases is about 5 wt%. The curves are shifted vertically for clarity.

evaporation. The vapor pressure of 1-hexadecene at 200 and 240 °C is approximately 10 and 35 kPa, respectively, while that for 1-heptadecene is 7.5 and 24 kPa, respectively, and that for 1-octadecene is 4.1 and 15.2 kPa, respectively [21]. For comparison, benzene has a vapor pressure of 15.8 kPa at 30 °C. On the other hand, during melt mixing, evaporation is minimal and the primary mechanism by which the degradation products leave the clay galleries should be dissolution into the matrix polymer. The α-olefins should be readily soluble in polyethylene, and so they are easily extracted from the clay galleries into the matrix polymer. This combined with possibly some effects of the mechanical forces generated during extrusion results in the collapsing of the clay galleries. A comparison of the WAXS patterns of LDPE-nanocomposites to that of pristine tetramethyl ammonium organoclay, M_4 (no alkyl tails), as shown in Fig. 11, supports the above theory. After the elimination of the α-olefins the organoclay *d*-spacing of the LDPE–$M_3(HT)_1$ nanocomposites approaches that of pristine M_4 organoclay (13.8 Å). X-ray scans of nanocomposites prepared by melt mixing poly(ethylene-*co*-methacrylic acid) ionomers with one-tailed organoclays at 200 °C exhibit similar patterns [14]. On the other hand, the α-olefins may not be as soluble in polypropylene as in polyethylene. This could explain why, under the same processing conditions, the WAXS peak for PP–$M_3(HT)_1$ composites is not shifted as much to the right as for the PE–$M_3(HT)_1$ composites (Fig. 11).

5. Conclusion

Surfactant degradation in melt processed polyethylene–organoclay nanocomposites was examined using WAXS and thermogravimetric analyses, and its effect on nanocomposite mechanical properties was evaluated using stress–strain analysis. Since polyethylene has a low melting point, it was possible to conduct this examination over a wide range of temperatures (150–240 °C). The *d*-spacing from the WAXS peaks for nanocomposites based on both $M_3(HT)_1$ and $M_2(HT)_2$, decreased by 3–4 Å when the processing temperature was raised from 180 to 200 °C, thus suggesting a sharp increase in the amount of surfactant leaving the organoclay galleries between these temperatures. The extent of surfactant degradation in the melt processed nanocomposites was determined to be independent of the organoclay content.

The improvement in tensile modulus resulting from melt mixing LDPE with $M_3(HT)_1$ organoclay was much less than for LDPE–$M_2(HT)_2$ nanocomposites, and the modulus seemed to be unaffected by the level of organoclay degradation. On the other hand, the relative modulus (E/E_m) of LDPE–$M_2(HT)_2$ nanocomposites dropped steadily as the processing temperature increased beyond 165 °C. It appears that depletion of organic material from the organoclay galleries by degradation and the resulting reduction in the interplatelet distances restricts the ability of LDPE to exfoliate the $M_2(HT)_2$ organoclay.

Thermogravimetric analysis of $M_3(HT)_1$, $M_2(HT)_2$ and $M_1(C_{16})_3$ organoclays suggest that organoclays based on surfactants with multiple alkyl tails have greater thermal stability than those based on surfactants with a single alkyl tail. The mass of surfactant lost during melt processing of nanocomposites was found to be greater than during thermogravimetric analysis of organoclays (in the absence of polymer). This could be attributed to the high solubility of the degradation products (predominantly α-olefins) in the polyethylene matrix, thus facilitating an easier removal of these products from the organoclay by extrusion as compared to TGA where the degradation products leave by evaporation.

Acknowledgements

This work was funded by the Air Force Office of Scientific Research. The authors sincerely thank Doug Hunter and Tony Gonzales of Southern Clay Products, Inc. for providing organoclay materials, WAXS data, and many helpful discussions. We are also thankful to Judy Webb-Barrett of Nova Chemicals for donating LDPE samples, and Chevron Phillips Chemical Company for providing the melt index measurements.

References

[1] Delozier DM, Orwoll RA, Cahoon JF, Johnston NJ, Smith JG, Connell JW. Polymer 2002;43(3):813–22.
[2] Fornes TD, Yoon PJ, Paul DR. Polymer 2003;44(24):7545–56.
[3] Yoon PJ, Hunter DL, Paul DR. Polymer 2003;44(18):5341–54.
[4] Matayabas Jr JC, Turner SR. In: Pinnavaia TJ, Beall GW, editors. Polymer–clay nanocomposites. New York, NY: Wiley; 2000. p. 207.
[5] Xie W, Gao Z, Pan W-P, Hunter D, Singh A, Vaia R. Chem Mater 2001; 13(9):2979–90.
[6] Xie W, Gao Z, Liu K, Pan WP, Vaia R, Hunter D, et al. Thermochim Acta 2001;367-368:339–50.
[7] VanderHart DL, Asano A, Gilman JW. Chem Mater 2001;13(10): 3796–809.

[8] VanderHart DL, Asano A, Gilman JW. Macromolecules 2001;34(12):3819–22.
[9] Osman MA, Ploetze M, Suter UW. J Mater Chem 2003;13(9):2359–66.
[10] Gelfer M, Burger C, Fadeev A, Sics I, Chu B, Hsiao BS, Si M, Rafailovich M, et al. Langmuir 2004;20(9):3746–58.
[11] Davis R, Gilman J, VanderHart D. Polym Degrad Stab 2003;79:111–21.
[12] Hotta S, Paul DR. Polymer 2004;45(22):7639–54.
[13] Shah RK, Paul DR, in preparation.
[14] Shah RK, Hunter DL, Paul DR. Polymer 2005;46(8):2646–62.
[15] Fornes TD, Yoon PJ, Hunter DL, Keskkula H, Paul DR. Polymer 2002;43(22):5915–33.
[16] Paul DR, Zeng QH, Yu AB, Lu GQ. J Colloid Interface Sci 2005;292(2):462–8.
[17] Yoon PJ, Hunter DL, Paul DR. Polymer 2003;44(18):5323–39.
[18] Shah RK, Paul DR. Polymer 2004;45(9):2991–3000.
[19] Fornes TD, Yoon PJ, Keskkula H, Paul DR. Polymer 2001;42(25):9929–40.
[20] Chavarria F, Paul DR. Polymer 2004;45(25):8501–15.
[21] DIPPR 801 database (http://dippr.byu.edu/).